Published in final edited form as:
Neuroscience. 2005 ; 136(3): 945–955.

QUANTITATIVE ASSESSMENT OF DEVELOPING AFFERENT PATTERNS IN THE CAT INFERIOR COLLICULUS REVEALED WITH CALBINDIN IMMUNOHISTOCHEMISTRY AND TRACT TRACING METHODS

C. K. Henkel[a,*], **M. L. Gabriele**[b], and **J. G. Mchaffie**[a]

a*Wake Forest University School of Medicine, Department of Neurobiology and Anatomy, Medical Center Boulevard, Winston-Salem, NC 27157, USA*

b*James Madison University, Department of Biology, Mathematics and Science College 7801, Harrisonburg, VA 22807, USA*

Abstract

The central nucleus of the inferior colliculus (CNIC) is comprised of an orderly series of fibrodendritic layers. These layers include integrative circuitry for as many as 13 different ascending auditory pathways, each tonotopically ordered. Calcium-binding proteins, such as calbindin-D28k (CB), may be useful neurochemical markers for specific subsets of afferent input in these layers and their spatial organization that are developmentally regulated. In this study, CB-immunohistochemistry was used to examine 1–42 postnatal-day-old kitten and adult cat CNIC and anterograde tracers were used to label afferent projections from the lateral superior olivary nucleus (LSO) to the CNIC at similar ages. A distinct axonal plexus that is CB-immunopositive is described. This CB-afferent compartment is present at birth and persists throughout the ages examined. Already at birth, the CB-immunostained plexus in kitten CNIC is organized into discrete bands that are approximately 75 μm thick and 500 μm long. In adult CNIC, the periodic banded pattern of CB-immunostained fibers is similar to that in kittens albeit bands are thicker (145 μm) and longer (700 μm). Growth in band thickness in adult cat appears proportional to growth of the IC, whereas length of the dense CB-immunostained bands is somewhat more focused in the central region of fibrodendritic layers. The banded pattern of the CB-immunostained plexus is well correlated with the location and dimension of afferent projections from the LSO in newborn kitten labeled with carbocyanine dye, 1,1′-dioctodecyl-3,3,3′,3′-tetramethylindocarbocyanine perchlorate and in adult cat labeled with wheat germ agglutinin conjugated with horseradish peroxidase. The results reveal a neurochemical marker for one type of synaptic compartment in CNIC layers, banding, that is organized before hearing onset in kittens, but that may undergo some postnatal pruning.

Keywords

fibrodendritic laminae; banding pattern; calcium-binding proteins; lateral superior olivary nucleus; carbocyanine dye

In the auditory midbrain, the inferior colliculus (IC) is comprised of a large, seemingly homogeneous, central nucleus (CNIC) surrounded by a complex and heterogeneous arrangement of several paracentral nuclei (Berman, 1968;Rockel and Jones, 1973a,b;Morest and Oliver, 1984). The principal cells of the CNIC have disk-shaped dendritic trees that are

*Corresponding author. Tel: +1-336-716-4379; fax: +1-336-716-4534. E-mail address: chenkel@wfubmc.edu (C. K. Henkel).

aligned in parallel with overlapping sheets of afferent fibers (Rockel and Jones, 1973a;Oliver and Morest, 1984). With only a few exceptions, all ascending hindbrain auditory pathways project to the CNIC and end in cochleotopic fashion within a series of these fibrodendritic layers. Overlaid on this network of hindbrain inputs are additional inputs from regions of auditory cortex and the contralateral IC as well as non-auditory structures (for review, see Oliver and Shneiderman, 1989). Less numerous are stellate cells and a subset of intrinsic axonal collaterals that depart from this laminar framework and cross laminar boundaries (Oliver et al., 1991).

Overall, the stereotypical structure of the CNIC belies the underlying complexity, intrinsic structure, and functional relationships within layers that are only evident with experimental intervention. Furthermore, development of complex synaptic domains that comprise the integrative circuitry of these layers remains largely unexplored. Several afferent projections to the CNIC have been shown previously to end along fibrodendritic layers in a pattern of bands and patches (Oliver and Shneiderman, 1989;Oliver et al., 1997). This afferent pattern predicts an intrinsic organization and possible modular compartmentalization that is not obvious with typical cytoarchitectural or histo-chemical staining. Other structural markers of this compartmentalization, however, remain to be elucidated that would provide powerful tools for assessment of the organization and functional processing within the IC.

We were particularly intrigued then by the possibility that calcium-binding protein markers might reveal aspects of segregation in layered circuits of the CNIC as well as providing insights into when and how such organization develops. Apart from their specific functional roles in calcium-buffering mechanisms, calcium-binding proteins have provided useful phenotypic markers for spatial patterns that may have important functional correlates within complex neuronal structures such as the IC. In a variety of brain regions, including sensory systems, calcium-binding proteins such as calbindin-D28k (CB), calretinin, and parv-albumin are distributed selectively within certain functional neuronal groups and their connections but not in others (Baimbridge et al., 1992;Andressen et al., 1993). Furthermore, in some instances, their expression is regulated developmentally (e.g. Lohmann and Friauf, 1996;Liu and Graybiel, 1992;Braun et al., 1988).

In this paper, we present analysis of the organization and postnatal development of an axonal plexus or compartment in the cat CNIC that is neurochemically defined by its CB-immunoreactivity. The spatial pattern of the CB-immunostained axons in the CNIC is compared in neonatal and adult animals with anterograde labeling of a banded projection from the lateral superior olivary nucleus (LSO) to the CNIC (Shneiderman and Henkel, 1987). Some preliminary findings from this study have been reported previously (McHaffie et al., 2000;Henkel et al., 2001;Brunso-Bechtold and Henkel, 2005).

EXPERIMENTAL PROCEDURES

Brains for this study were obtained from five adult cats and 10 kittens (1, 4, 8, 11, 15, 28, and 42 postnatal-days-old (P)). All animal care and experimental procedures were carried out so as to minimize the number of animals used and any pain or suffering and were in compliance with the Guide for the Care and Use of Laboratory Animals in facilities accredited by the American Association for the Accreditation of Laboratory Animal Care (AAALAC). Experimental protocols were approved by the Institutional Animal Care and Use Committee at Wake Forest University School of Medicine (Winston-Salem, NC, USA). Animals were sedated with ketamine hydrochloride (10 m/kg) and administered 1.0 ml heparin. Twenty minutes later, they were deeply anesthetized with sodium pento-barbital (100 mg/kg) and perfused transcardially with 0.9% saline followed by a fixative solution containing 4% paraformaldehyde and 0.1% glutaraldehyde in 0.1 M sodium phosphate buffer, pH 7.4 for 1–

2 h. The brains were stereotaxically blocked *in situ*, removed from the skull, and stored overnight at 4 °C in 0.1 M phosphate buffer. Coronal sections were cut at 50 μm thickness on a Vibratome™ (Technical Products International, St. Louis, MO, USA).

Immunohistochemistry

In these experiments, tissue was processed for detection of CB using the avidin–biotin peroxidase complex immunohistochemical method (Hsu et al., 1981). Briefly, free-floating sections were washed with phosphate-buffered saline, pH 7.2. To reduce nonspecific binding, sections were blocked for 1 h in 10% normal horse serum in phosphate-buffered saline containing 1% Triton X-100, 1% bovine serum albumin, and 0.1 M L-lysine at room temperature. Sections were then incubated in a 1:400 dilution of the CB primary antibody (Sigma, St. Louis, MO, USA) containing 1% normal horse serum and 0.1% Triton X-100 in phosphate-buffered saline for 12–14 h at room temperature with constant agitation. Sections were rinsed three times with 1% normal horse serum and then immersed in biotinylated anti-mouse IgG diluted 1:250 in phosphate-buffered saline for 60 min at room temperature.

Following exposure to the biotinylated secondary antibody, sections were washed in three 10-min phosphate-buffered saline rinses and incubated with avidin–biotin–peroxidase (Vector Laboratories, Burlingame, CA, USA) for 60 min. Sections were stained with peroxidase histochemistry using diaminobenzidine (DAB) as the substrate for a brown reaction product or DAB and nickel-cobalt intensification for a black reaction product. After several rinses in 0.1 M phosphate buffer, sections were mounted on gelatin-coated glass slides, dehydrated with a graduated alcohol/xylene series, and coverslipped with Permount (Fisher Scientific, Pittsburgh, PA, USA). Control sections for nonspecific binding underwent the same experimental procedure except for the omission of primary antibody in the first overnight exposure. Companion serial sections from each case were treated with antibodies against other calcium-binding proteins (calretinin, parvalbumin), presented differential staining in the IC from that with CB, and will be described in subsequent reports.

Neonate anterograde tracing: carbocyanine dyes

In a series of six kittens, P1–P9, axonal projections of the LSO to the CNIC were traced using the carbocyanine dye, 1,1′-dioctodecyl-3,3,3′,3′-tetramethylindocarbocyanine perchlorate (DiI). Briefly, the animals were perfused with 4% paraformaldehyde in phosphate buffer. The brains were removed, blocked in the coronal plane, and postfixed overnight in the same fixative in the refrigerator. To position a DiI-coated pin in the LSO, the medulla was sectioned on the Vibratome until the interface of the facial motor nucleus and LSO was reached. Fine, glass filaments coated with DiI (Molecular Probes, Eugene, OR, USA; Vibrant DiI D-282) were carefully inserted at right angle to the face of the block into the emerging LSO. The blocks were returned to fresh fixative and incubated in the dark at 37 °C for 1.5–6 months. After incubation, the blocks were embedded in egg yolk, sectioned on the Vibratome at 75 μm thickness, mounted on glass slides, and coverslipped using Gel Mount (Biomeda, Foster City, CA, USA).

Adult anterograde tracing: wheat germ agglutinin conjugated with horseradish peroxidase (WGA-HRP)

A large collection of cases from a previous study with WGA-HRP injections in the adult cat LSO was utilized to analyze the pattern of afferent projections to the IC. The methods have been described in more detail previously (Shneiderman and Henkel, 1987). Briefly, a 5–25 nl injection of 1% WGA-HRP (Sigma) was placed stereotaxically in the LSO. The animals survived 1–7 days before being perfused with 1% paraformaldehyde and 2.5% glutaraldehyde in normal buffered saline. The brains were removed from the skull, blocked in the stereotaxic

coronal plane, frozen, and sectioned at 50 μm thickness. Peroxidase histochemistry using tetramethylbenzidine as the substrate was used to detect the tracer in the sections.

Microscopic analysis and photography

Images for analysis were captured using an Olympus BX2 photomicroscope (Melville, NY, USA) and Spot RT Slider color digital camera (Diagnostic Instruments, Sterling Heights, MI, USA). Density profiles of immunopositive regions were obtained using Scion Image software (Scion Corporation, Frederick, MD, USA) and analyzed with GraphPad Prism (GraphPad Software, San Diego, CA, USA). The method for analysis of line density functions has been described in detail previously (Henkel et al., 2003). Data were collected for three cases with the best staining or labeling in each group. Briefly, two to three sections through the middle of dense labeling were identified and digital images of CNIC were smoothed with a Gaussian filter. Scion Image software was used to measure the gray levels along a line through the immunostained or labeled plex-uses at approximately right angle to the fibrodendritic layers of the CNIC. The peaks and troughs of this line function represented dense and light bands of immunostaining or labeling. The data for each line function were transferred to an Excel spreadsheet (Microsoft, Redmond, WA, USA) and analyzed with GraphPad Prism. In this way, six to 12 peaks were measured in each of three cases. Actual band size in each group is expressed as the mean and standard deviation in microns. The lengths of immunostained bands in the frontal plane were measured based on similar analysis of density functions along the plane of the layers. Measurements at different ages were compared using Student's *t*-test and *P* values less than 0.05 were considered statistically different. To normalize measurements in different ages for general brain growth, measurements of thickness and length were expressed as a ratio of IC size. Since the diameter of the IC or its CNIC varied in different planes, the entire IC was outlined to determine the area and the square root of the area was used as a linear index of IC size (Leake et al., 2002). Henceforth, this is simply referred to as the IC linear size index expressed in microns and the ratio of thickness or length of bands to diameter as the normalized or relative size.

Working measure of the CNIC

The nomenclature of subdivisions of the IC has varied in cytoarchitectural studies. Morest and Oliver (1984) described the cat IC as comprising tectal and tegmental regions based on rapid Golgi staining of cells and axons. The tectal component they described consisted of a large, CNIC characterized by its predominant disk-shaped cells, a cortex (both dorsal and caudal to the CNIC), and various paracentral nuclei. Here we use that classification to organize our description of CB-immunostaining. For clarity it should be pointed out that the lateral nucleus of the IC according to this schema corresponds basically in alternate nomenclature to the external nucleus or cortex (ECIC) and superficial layers of dorsal cortex of the inferior colliculus (DCIC) to the pericentral nucleus of the IC (Berman, 1968;Rockel and Jones, 1973b).

RESULTS

CB-immunostained afferent compartment in CNIC in neonatal kitten

At birth (P1), about a week before hearing onset in kittens (Shipley et al., 1980;Walsh and McGee, 1987), a dense afferent plexus in the IC was immunostained for CB (Fig. 1). There was a decreasing gradient in distribution of CB-immunostained cells from the superficial layers to the deep layers of the DCIC that continued into the central region of IC (Zettel et al., 1991;Kelley et al., 1992;Friauf, 1994;Forster and Illing, 2000). In contrast, the dense plexus of heavily CB-immunostained axonal fibers and endings was centered in CNIC and did not extend significantly toward paracentral regions (see CNIC in Fig. 1). Many CB-immunostained

axons entered the ventral region of the CNIC from the lateral lemniscus, whereas few were found in the commissure of the IC.

The distribution of the CB-plexus in the neonatal CNIC was not uniform. The plexus was denser in the ventromedial two-thirds of the CNIC than in the dorsolateral region. In the ventromedial plexus, CB-immunostained fibers and endings were distributed along parallel layers but with obvious discontinuities between and along layers. Most notably, many fibers and endings formed a series of heavily immunostained bands separated by parallel regions with less dense CB-immunostaining (Fig. 2). The thickness and the length of CB-immunostained bands formed by the plexus varied within a section as well as between sections from different rostral–caudal sectors of the CNIC.

Postnatal changes in the CB-immunostained afferent compartment

Although density of CB-immunostained fibers along the length and breadth of the afferent plexus varied, banding appeared to be a regular pattern in the central part of CNIC in each animal and age examined (Fig. 3). CB-immunostaining was prominent in small punctate endings as well as pre-terminal fibers. Since CB-immunostained cells were infrequent in CNIC relative to their prominent distribution in surrounding paracentral nuclei (see superficial and deep layers of DCIC in Fig. 1), few dendritic profiles contributed to this plexus (Fig. 2). As a measure of the periodicity in CB-immunostaining, image gray level density was plotted along a line intersecting the midregion of layers in CNIC as shown in detail in Fig. 4. These line plots were used to calculate band thickness at half the height of the peaks. A regular periodicity in the pattern of banded immunostaining was indicated by the larger R^2 for best curve fit with a sine wave (non-linear regression analysis) in the ventromedial region (Fig. 4a, b, e) compared with the dorsolateral region of the CNIC (Fig. 4a, b, f). In neonatal CNIC (Fig. 5A), peaks in the line density plots representing CB-immunostained afferent bands were about 76±3 μm thick (N=3). A similar measure parallel to the ventrolateral–dorsomedial axis of the layers (Fig. 6A) indicated that bands occupied a segment of IC layers that was 526±79 μm long (N=3).

There was little change in the overall appearance of CB-immunostained afferent bands in IC for each of the older postnatal ages examined (P4, P8, P11, P15, P21, P28, P42; Fig. 3) and for adults (Fig. 1B). In adult cats, the blanket of CB-immunostained fibers extended over almost the entire CNIC. In the middle and ventral part of CNIC, the densest region of CB-immunostained fibers was distributed centrally in bands and patches with only scattered fibers extending dorsomedially into the deepest layer of DCIC. From line density plots through the immunostained plexus, bands of CB-immunostained fibers and endings were 144±6 μm thick (N=3) and 705±67 μm long (N=3) in adult CNIC (Figs. 5A and 6A respectively), significantly greater than similar measures in neonatal CNIC. Dorsolaterally, some CB-immunostained fibers and endings in adult cats occupied a patchy region that extended into DCIC but that was not very dense laterally at the border with ECIC. In general, this dorsolateral region of CB-immunostaining lacked the banded organization seen more centrally and ventromedially in the CNIC.

Growth or maintenance of CB-bands relative to IC growth

In order to compare the size and distribution of the banded regions of the CB-immunostained plexus in the CNIC at different ages, measures of band thickness and length were normalized with respect to a linear index of IC size. Not surprisingly banded regions in the CB-immunostained plexus increased in dimensions with general growth of the IC, but with some differences. The normalized values for band thickness in adult CNIC (0.031±0.001) and in neonates (0.031±0.003) were similar as shown in Fig. 5B. On a qualitative level it appeared that interband regions contained even less CB-immunostaining overall in older postnatal animals and adults than in neonates (Fig. 2A, B), suggesting that refinement of afferent bands

in this dimension may occur without overall change in the thickness of the afferent bands. Thus, the periodicity in density was similar for all ages examined. In contrast to band thickness, normalized band length (see Fig. 6B) was actually significantly shorter for adult CB-immunostained afferents (0.15±0.14%) than for neonates (0.21±0.09) suggesting that segregation of CB-endings in afferent zones became more concentrated in the central segment of IC layers as afferent circuits matured.

Comparison of LSO bands with CB-afferent compartment

A survey of brainstem auditory nuclei in the CB-immunostained material indicated that projection cells in LSO and portions of ventral nucleus of the lateral lemniscus might contribute to such a CB-immunostained afferent plexus (see Zettel et al., 1991;Kelley et al., 1992;Friauf, 1994;Forster and Illing, 2000). There were no CB-immunostained projection cells in other nuclei such as DNLL and dorsal cochlear nucleus that previously have been shown to give rise to banded projections in the CNIC (see Oliver and Shneiderman, 1989 for review). LSO has been shown previously to end in a series of afferent bands in adult cat IC that interdigitate with similar bands from the same nucleus on the other side (Shneiderman and Henkel, 1987). Given these relationships of afferent organization and CB-immunostaining, the distribution and growth of LSO-afferent projections were compared with the pattern of the CB-immunostained axons.

Anterograde tracers labeled LSO projections to the IC in neonatal kittens (P1, P6, P9) and in adult cats (see Fig. 7 A, B and C, D, respectively). As expected the pattern of axonal distribution in both age groups resembled the banded CB-afferent compartment at these ages. DiI-labeled bands in neonatal kittens were 77±11 μm thick and 573±91 μm long (Figs. 5A and 6A, respectively). WGA-HRP-labeled bands in adult cats were 157±11 μm thick and 673±99 μm long (Figs. 5A and 6A, respectively). Statistical comparison of LSO-afferent projections to CNIC showed that both band thickness (Fig. 5B) and band length (Fig. 6B), when normalized for tissue shrinkage, were not significantly different than similar measures for the CB-afferent plexus of the same age group.

DISCUSSION

The results show that CB immunostaining in CNIC includes an afferent plexus distributed in distinct bands parallel to fibrodendritic layers. CB bands are present at birth in kittens as well as in adult cats. Compared with CB bands in kittens, adult CB bands increase markedly in thickness, but are only slightly longer. However, these changes in CB band thickness and length differ significantly relative to overall IC growth. On the one hand, as IC size increases, relative band thickness and spacing are maintained. On the other hand, relative length of bands becomes shorter in adult IC than in neonate IC, suggesting pruning in that dimension of the afferent plexus or some differential growth of IC subnuclei. The dimensions and spacing of LSO bands labeled with the carbocyanine dye, DiI as an anterograde tracer in neonatal kittens or WGA-HRP in adult cat were similar to dimensions of CB bands. Thus, CB immunostaining reveals a neurochemically defined afferent compartment within CNIC. Developmental changes in CB afferent bands are likely to correspond to maturing circuitry that integrates ascending information from binaural pathways such as that from LSO, activated once hearing begins by interaural level differences, with other functional inputs.

Calcium binding proteins have proven useful as neurochemical markers of afferent patterns in a variety of brain regions, including the cat IC (e.g. Chernock et al., 2004). In CNIC, a distinct afferent domain has been described for calretinin-immunopositive fibers. Calretinin immunostaining appears to be a neurochemical marker for the medial superior olivary nucleus (MSO) projections to the IC in birds (Takahashi et al., 1987) and most likely in mammals (Fuentes-Santamaria et al., 2003;Alvarado et al., 2004) as well, although other inputs may be

included that occupy overlapping domains. The location and pattern of distribution of CB correspond to afferent inputs to the CNIC from LSO. Thus, a powerful approach to dissect the functional organization of integrative circuits in the auditory midbrain would be to combine this neurochemical marker with other anatomical methods or electrophysiological recordings to reveal specific properties common to CB domains of the fibrodendritic layers of the CNIC.

Furthermore, a number of developmental studies of calcium binding proteins in the auditory as well as other systems show their usefulness as spatiotemporal markers of developing circuitry (e.g. auditory brainstem nuclei, Lohmann and Friauf, 1996; striatum, Liu and Graybiel, 1992; vocal nuclei, Braun et al., 1988; barrel fields of somatosensory cortex, Melvin and Dyck, 2003). In particular, calcium-binding proteins are differentially distributed within LSO during development with calretinin-immunostaining being present at high levels in core LSO neurons that project to the contralateral IC and calbindin (and parvalbumin) being present in shell LSO neurons that project to the ipsilateral IC (Henkel and Brunso-Bechtold, 1998). Further study is required to show how this differential distribution of calcium-binding proteins might be related to early activity and refinement of these developing circuits.

Developmental plasticity of auditory circuitry has been shown in a variety of mammalian and non-mammalian brainstem auditory nuclei. For instance, axonal arbors from cells in the medial nucleus of the trapezoid body first distribute some aberrant branches and endings widely across the tonotopic axis in postnatal gerbil LSO before being pruned to match the narrower domain of the adult LSO (Sanes and Siverls, 1991). Similarly, initially exuberant dendritic arbors in chick nucleus laminaris (Smith and Rubel, 1979), gerbil and ferret MSO and LSO (Henkel and Brunso-Bechtold, 1990,1991;Sanes et al., 1992;Sanes and Friauf, 2000), and rat and cat IC (Meininger and Baudrimont, 1981;Dardeness et al., 1984;Gonzalez-Hernandez et al., 1989) eventually become restricted to flattened or disk-like domains. Such shaping or sculpting of presynaptic and postsynaptic elements establishes precise synaptic domains related to frequency processing.

That CB bands are already present at birth indicates that this particular integrative pattern in kittens develops prior to hearing onset which is generally at the end of the first postnatal week (Shipley et al., 1980;Walsh and McGee, 1987). Interestingly, using rapid Golgi staining to study the architecture of kitten IC, Gonzalez-Hernandez et al. (1989) showed a similar pattern of dense and light bands with the dense bands being comprised of a network of axonal and dendritic profiles. In fact, other developmental studies indicate that brainstem auditory projections to the IC develop remarkably early, well before functional hearing and any role for sensory experience. For instance, Kandler and Friauf (1993) showed that cochlear nucleus projections to the contralateral IC reach their targets prenatally and are well refined even by birth. Also, in ferret kits, an altricial carnivore that does not hear until 1 month postnatally, the relative laterality of the LSO inhibitory projections to the ipsilateral IC and excitatory projections to the contralateral IC are already established at birth (Henkel and Brunso-Bechtold, 1993). LSO projections to CNIC have been studied in adult cat (Shneiderman and Henkel, 1987;Oliver et al., 1997), are distinctly banded in their distribution, and occupy alternating sublayers, that is, interdigitate with their counterparts from the opposite LSO. As for CB bands in cat IC, these LSO bands already may be in place in ferret IC before hearing onset (Brunso-Bechtold and Henkel, 2005). Finally, Gabriele et al. (2000a) showed that in rat inhibitory projections to the contralateral IC from the dorsal nucleus of the lateral lemniscus (DNLL) have invaded IC by birth and subsequently form a banded pattern parallel to CNIC layers 3–4 days before hearing onset. In the latter example (Gabriele et al., 2000a), DNLL afferents initially proliferate within a large expanse of CNIC. Afferent axons become more restricted in their branching so as to conform to the domain of a fibrodendritic layer. Eventually patches form that are shorter in length than the initial bands described. Sculpting of the pattern of CB bands in kitten CNIC appears to be similar in that bands once formed are pruned to fit

within a short patch along the longer dimension of the fibrodendritic layers with which they are co-aligned. Similar changes in the length of afferent bands were observed for developing DNLL projections to the neonatal rat IC (Gabriele et al., 2000a). These spatiotemporal changes are likely to reflect, in part, competitive interactions that determine functional synaptic domains integrating specific sets of afferent inputs in IC circuitry (Oliver and Shneiderman, 1989).

The overall pattern of CB immunostaining is strikingly reminiscent of other mosaic patterns in sensory regions such as ocular dominance stripes in visual cortex (see Crowley and Katz, 2000,2002 for reviews) and whisker barrel fields in somatosensory cortex (see Petersen, 2003 for review). Furthermore, calcium binding proteins are among the various markers of these developing patterns (e.g. Yan et al., 1995;Melvin and Dyck, 2003). Considerable experimental evidence exists supporting a role for competitive interactions of inputs from the periphery in establishing or maintaining the mosaic patterns in visual and somatosensory cortex. Presumably, similar mechanisms guide assembly of IC circuits, although much remains to be learned about how ascending pathways from as many as 13 different major auditory brainstem nuclei (see review by Oliver and Shneiderman, 1989) are appropriately aligned. Support for this hypothesis was demonstrated by a previous study (Gabriele et al., 2000b). In that study, DiI placed in the commissure of Probst labeled crossed projections from the DNLL to the rat CNICs. Following early, postnatal unilateral cochlear ablation, symmetry of the periodic banded patterns was disrupted. Thus, early neural activity, whether evoked or spontaneous, is likely to be involved at some level in development of integrative circuits in this complex structure.

Acknowledgments

Supported by DC 04412, DC 00813, NS 36916 and NS 35008.

Abbreviations

CB, calbindin-D28k; CNIC, central nucleus of the inferior colliculus; DAB, diaminobenzidine; DCIC, dorsal cortex of the inferior colliculus; DiI, 1,1′-dioctodecyl-3,3,3′,3′-tetramethylindocarbocyanine perchlorate; DNLL, dorsal nucleus of the lateral lemniscus; ECIC, external cortex of the inferior colliculus; IC, inferior colliculus; LSO, lateral superior olivary nucleus; MSO, medial superior olivary nucleus; P, postnatal day; WGA-HRP, wheat germ agglutinin–horseradish peroxidase.

REFERENCES

Alvarado JC, Fuentes-Santamaria V, Henkel CK, Brunso-Bechtold JK. Alterations in calretinin immunostaining in the ferret superior olivary complex after cochlear ablation. J Comp Neurol 2004;470:63–79. [PubMed: 14755526]

Andressen C, Blümcke I, Celio MR. Calcium-binding proteins: Selective markers of nerve cells. Cell Tissue Res 1993;271:181–208. [PubMed: 8453652]

Baimbridge KE, Celio MR, Rogers JH. Calcium-binding proteins in the nervous system. Trends Neurosci 1992;15:303–308. [PubMed: 1384200]

Berman, AL. A cytoarchitectonic atlas with stereotaxic coordinates. The University of Wisconsin Press; Madison, WI: 1968. The brain stem of the cat.

Braun K, Scheich H, Zuschratter W, Heizmann CW, Matute C, Streit P. Postnatal development of parvalbumin-, calbindin- and adult GABA-immunoreactivity in two visual nuclei of zebra finches. Brain Res 1988;475:205–217. [PubMed: 3214731]

Brunso-Bechtold, JK.; Henkel, CK. Development of auditory afferents to the central nucleus of the inferior colliculus. In: Winer, JA.; Schreiner, CE., editors. The inferior colliculus. Springer-Verlag; New York: 2005. p. 537-558.

Chernock ML, Larue DT, Winer JA. A periodic network of neurochemical modules in the inferior colliculus. Hear Res 2004;188:12–20. [PubMed: 14759566]

Crowley JC, Katz LC. Early development of ocular dominance columns. Science 2000;290:1321–1324. [PubMed: 11082053]

Crowley JC, Katz LC. Ocular dominance development revisited. Curr Opin Neurobiol 2002;12:104–109. [PubMed: 11861172]

Dardeness R, Jarreau PH, Meiniger V. A quantitative Golgi analysis of the postnatal maturation of dendrites in the central nucleus of the inferior colliculus of the rat. Brain Res 1984;318:159–169. [PubMed: 6498496]

Forster CR, Illing RB. Plasticity of the auditory brainstem: Cochleotomy-induced changes of calbindin-D28k expression in the rat. J Comp Neurol 2000;416:173–187. [PubMed: 10581464]

Friauf E. Distribution of calcium-binding protein calbindin-D28k in the auditory system of adult and developing rats. J Comp Neurol 1994;349:193–211. [PubMed: 7860778]

Fuentes-Santamaria V, Alvarado JC, Brunso-Bechtold JK, Henkel CK. Upregulation of calretinin immunostaining in the ferret inferior colliculus after cochlear ablation. J Comp Neurol 2003;460:585–596. [PubMed: 12717716]

Gabriele ML, Brunso-Bechtold JK, Henkel CK. Development of afferent patterns in the inferior colliculus of the rat: projection from the dorsal nucleus of the lateral lemniscus. J Comp Neurol 2000a;416:368–382. [PubMed: 10602095]

Gabriele ML, Brunso-Bechtold JK, Henkel CK. Plasticity in the development of afferent patterns in the inferior colliculus of the rat after unilateral cochlear ablation. J Neurosci 2000b;20:6939–6949. [PubMed: 10995838]

Gonzalez-Hernandez TH, Meyer G, Ferres-Torres R. Development of neuronal types and laminar organization in the central nucleus of the inferior colliculus in the cat. Neuroscience 1989;30:127–141. [PubMed: 2747909]

Henkel CK, Brunso-Bechtold JK. Dendritic morphology and development in the ferret medial superior olivary nucleus. J Comp Neurol 1990;294:377–388. [PubMed: 2341617]

Henkel CK, Brunso-Bechtold JK. Dendritic morphology and development in the ferret lateral superior olivary nucleus. J Comp Neurol 1991;313:259–272. [PubMed: 1765583]

Henkel CK, Brunso-Bechtold JK. Laterality of superior olive projections to the inferior colliculus in adult and developing ferret. J Comp Neurol 1993;331:458–468. [PubMed: 8509504]

Henkel CK, Brunso-Bechtold JK. Calcium-binding proteins and GABA reveal spatial segregation of cell types within the developing lateral superior olivary nucleus of the ferret. Microsc Res Tech 1998;41:234–245. [PubMed: 9605341]

Henkel CK, Gabriele ML, McHaffie JG. Calcium-binding protein immunohistochemistry reveals afferent patterns in the inferior colliculus (IC) of adult cat. Soc Neurosci Abstr 2001;27Program No. 930.11

Henkel CK, Fuentes-Santamaria V, Alvarado JC, Brunso-Bechtold JK. Quantitative measurement of afferent layers in the ferret inferior colliculus: DNLL projections to sublayers. Hear Res 2003;177:32–42. [PubMed: 12618315]

Hsu SM, Raine L, Fanger H. Use of avidin-biotin peroxidase complex (ABC) in immunoperoxidase techniques: A comparison between ABC and unlabeled antibody (PAP) procedures. J Histochem Cytochem 1981;29:577–580. [PubMed: 6166661]

Kandler K, Friauf E. Pre- and postnatal development of efferent connections of the cochlear nucleus in the rat. J Comp Neurol 1993;328:161–184. [PubMed: 8423239]

Kelley PE, Frisina RD, Zettel ML, Walton JP. Differential calbindin-like immunoreactivity in the brain stem auditory system of the chinchilla. J Comp Neurol 1992;320:196–212. [PubMed: 1619049]

Leake PA, Snyder RL, Hradek GT. Postnatal refinement of auditory nerve projections to the cochlear nucleus in cats. J Comp Neurol 2002;448:6–27. [PubMed: 12012373]

Liu F-C, Graybiel AM. Heterogeneous development of calbindin-D_{28K} expression in the striatal matrix. J Comp Neurol 1992;320:304–322. [PubMed: 1351896]

Lohmann C, Friauf E. Distribution of the calcium-binding proteins parvalbumin and calretinin in the auditory brainstem of adult and developing rats. J Comp Neurol 1996;367:90–109. [PubMed: 8867285]

McHaffie JG, Gabriele ML, Stein BE, Wallace MT, Henkel CK. Banded distribution of calbindin D-28k immunoreactivity in the auditory brainstem of neonatal and adult cats. Soc Neurosci Abstr 2000;26:676.

Meininger V, Baudrimont M. Postnatal modifications of the dendritic tree of cells in the inferior colliculus of the cat. J Comp Neurol 1981;200:339–355. [PubMed: 7276243]

Melvin NR, Dyck RH. Developmental distribution of calretinin in mouse barrel cortex. Brain Res Dev Brain Res 2003;143:111–114.

Morest DK, Oliver DL. The neuronal architecture of the inferior colliculus in the cat: defining the functional anatomy of the auditory midbrain. J Comp Neurol 1984;222:209–236. [PubMed: 6699208]

Oliver DL, Morest DK. The central nucleus of the inferior colliculus in the cat. J Comp Neurol 1984;222:237–264. [PubMed: 6699209]

Oliver, DL.; Shneiderman, A. The anatomy of the inferior colliculus: a cellular basis for integration of monaural and binaural information. In: Altschuler, RA.; Bobbin, RP.; Clopton, BM.; Hoffman, DW., editors. Neurobiology of hearing: the central auditory system. Raven Press; New York: 1989. p. 195-222.

Oliver DL, Kuwada S, Yin TC, Haberly LB, Henkel CK. Dendritic and axonal morphology of HRP-injected neurons in the inferior colliculus of the cat. J Comp Neurol 1991;303:75–100. [PubMed: 2005240]

Oliver DL, Beckius GE, Bishop DC, Kuwada S. Simultaneous anterograde labeling of axonal layers from lateral superior olive and dorsal cochlear nucleus in the inferior colliculus of cat. J Comp Neurol 1997;382:215–229. [PubMed: 9183690]

Petersen CC. The barrel cortex-integrating molecular, cellular and systems physiology. Pflugers Arch 2003;447:126–134. [PubMed: 14504929]

Rockel AJ, Jones EG. The neuronal organization of the inferior colliculus of the adult cat. I: The central nucleus. J Comp Neurol 1973a;147:11–60. [PubMed: 4682181]

Rockel AJ, Jones EG. The neuronal organization of the inferior colliculus of the adult cat. II. The pericentral nucleus. J Comp Neurol 1973b;149:301–334. [PubMed: 4123504]

Sanes DH, Siverls V. Development and specificity of inhibitory terminal arborizations in the central nervous system. J Neurobiol 1991;22:837–854. [PubMed: 1663990]

Sanes DH, Song J, Tyson J. Refinement of dendritic arbors along the tonotopic axis of the gerbil lateral superior olive. Brain Res Dev Brain Res 1992;67:47–55.

Sanes DH, Friauf E. Development and influence of inhibition in the lateral superior olivary nucleus. Hear Res 2000;147:46–58. [PubMed: 10962172]

Shipley C, Buchwald JS, Norman R, Guthrie D. Brain stem auditory evoked response development in the kitten. Brain Res 1980;182:313–326. [PubMed: 7357388]

Shneiderman A, Henkel CK. Banding of lateral superior olivary nucleus afferents in the inferior colliculus: a possible substrate for sensory integration. J Comp Neurol 1987;266:519–534. [PubMed: 2449472]

Smith DJ, Rubel EW. Organization and development of brainstem and auditory nuclei of the chicken: dendritic gradients in N. laminaris. J Comp Neurol 1979;186:213–240. [PubMed: 447882]

Takahashi TT, Carr CE, Brecha NC, Konishi M. Calcium binding protein-like immunoreactivity labels the terminal field of nucleus laminaris of the barn owl. J Neurosci 1987;7:1843–1856. [PubMed: 2439666]

Walsh EJ, McGee J. Postnatal development of auditory nerve and cochlear nucleus neuronal responses in kittens. Hear Res 1987;28:97–116. [PubMed: 3610862]

Yan YH, van Brederode JF, Hendrickson AE. Transient co-localization of calretinin, parvalbumin, and calbindin-D28K in developing visual cortex of monkey. J Neurocytol 1995;24:825–837. [PubMed: 8576712]

Zettel ML, Carr CE, O'Neill WE. Calbindin-like immunoreactivity in the central auditory system of the mustached bat, Pteronotus parnelli. J Comp Neurol 1991;313:1–16. [PubMed: 1761747]

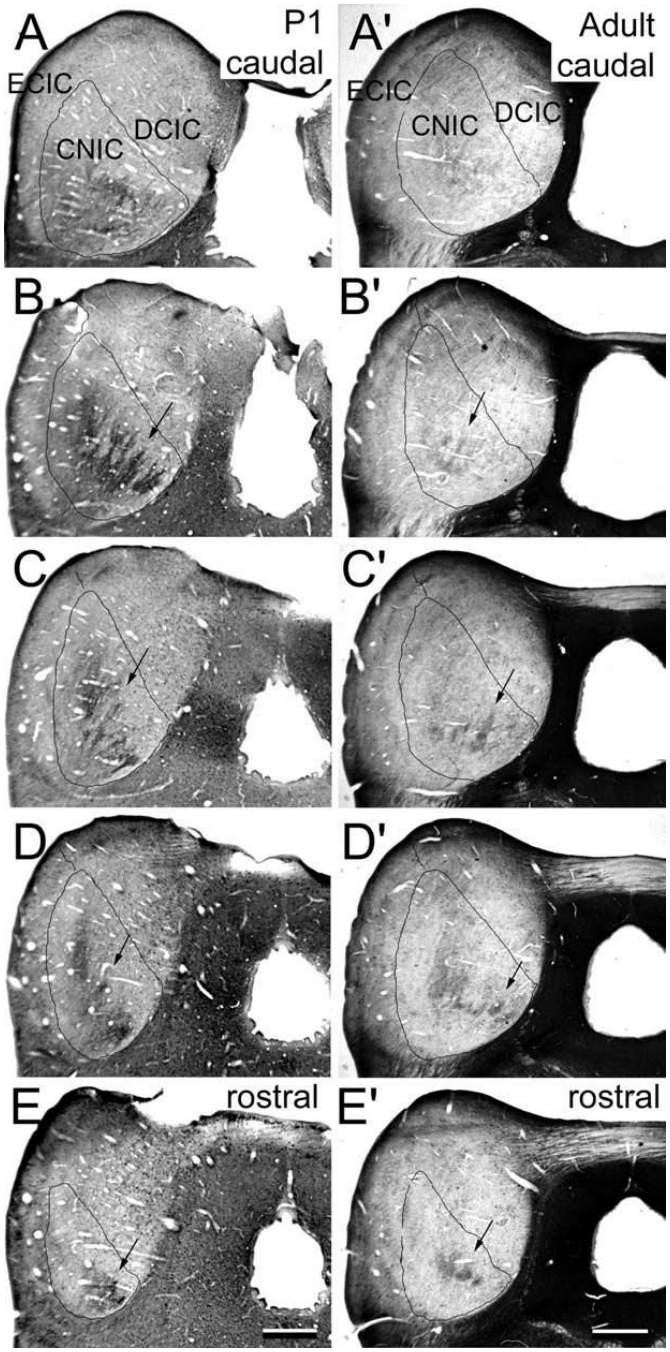

Fig 1.

Low magnification photomicrographs of CB-immunostaining in neonatal (P1) IC (left panel, A–E) and adult IC (right panel, A′–E′). Each panel shows a caudal (top) to rostral (bottom) series of frontal sections. The dense banded staining (see arrows) in each section is confined to the CNIC. Other immunostaining in the superficial layers of the DCIC and periaqueductal gray matter includes dense neuropil and cellular staining. Scale bars=0.5 mm, left panel; 1 mm, right panel. The CNIC is outlined and the main subnuclei of the IC are labeled in frames A, A ′ for reference.

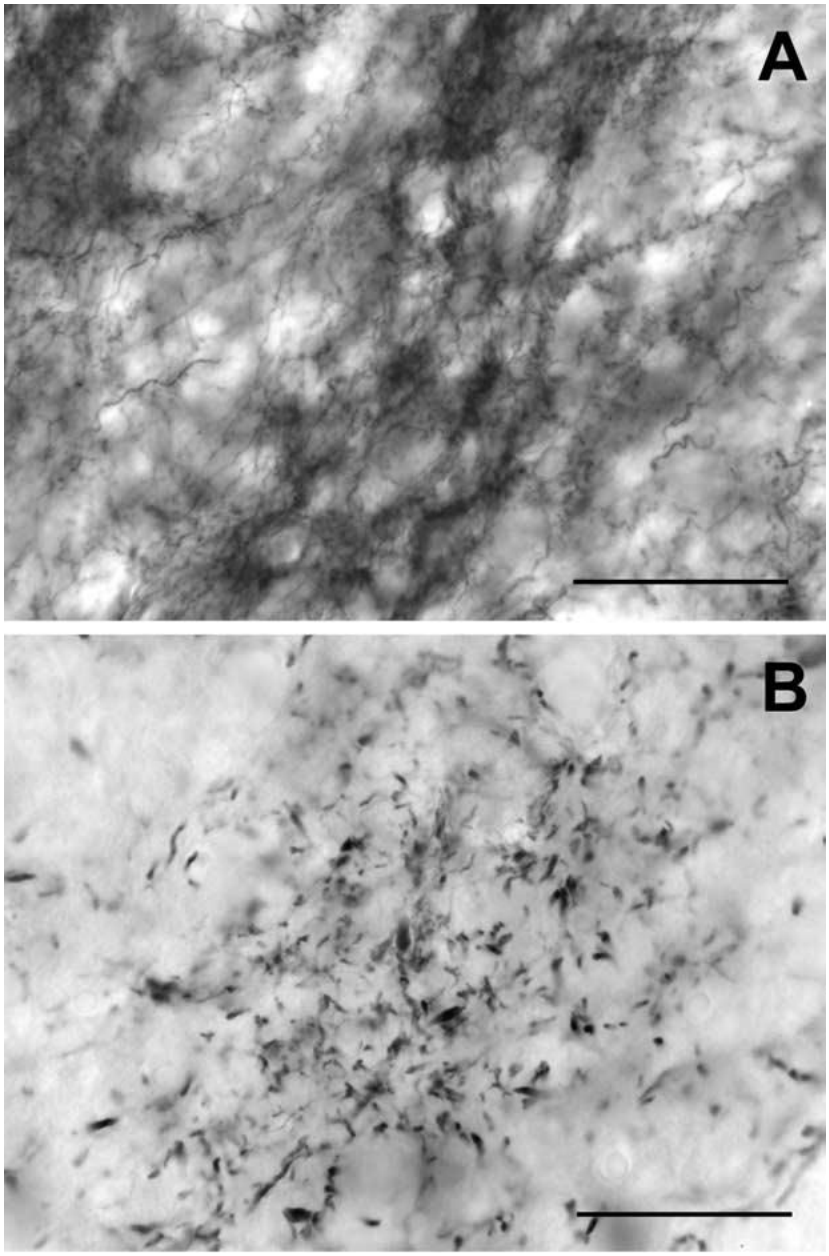

Fig 2.

Higher magnification digital photomicrographs of CB-immunostained bands showing complement of immunostained elements within and between banded regions of the afferent plexus in neonate and adult IC. (A) P1 calbindin bands (50× plan apo oil objective). CB-immunostaining is located in thin fibers and endings that are densely distributed within the band but less densely in bordering interband spaces. (B) Adult calbindin bands (50× plan apo oil objective). Small, punctate endings and thin preterminal axons comprise most of the dense labeling in adult CB bands and the interband areas contain almost no immunostained elements. Scale bars=50 μm.

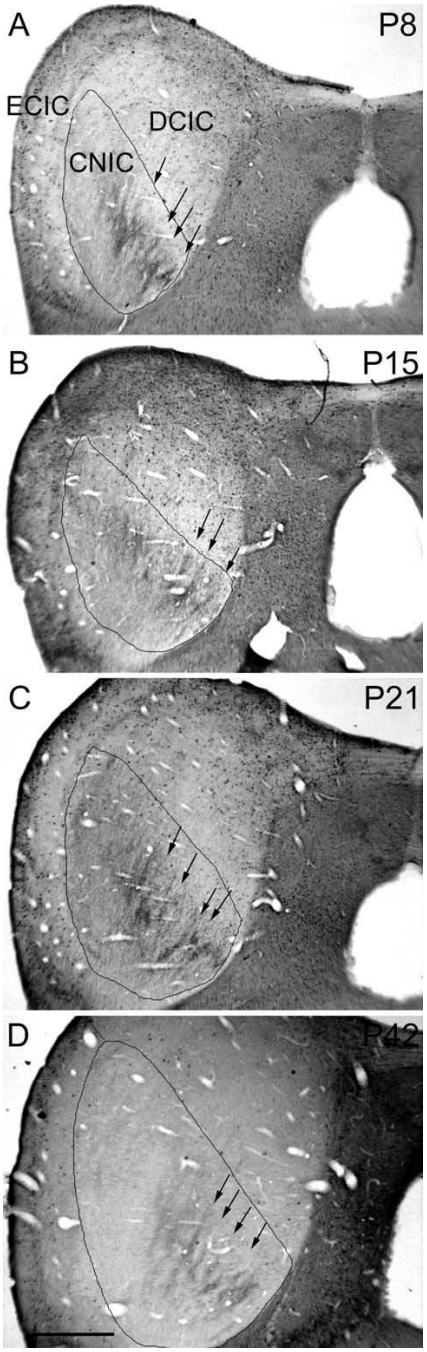

Fig 3.

Low magnification photomicrographs illustrating CB-immunostaining in a series of postnatal kitten. Bands (see arrows) are regularly displayed in the pattern of CB-immunostaining at each of the four post-natal ages. At this magnification, developmental changes in surrounding cellular staining are barely apparent. The CNIC is outlined and the main subnuclei of IC are labeled in frame A for reference. Scale bar=0.5 mm.

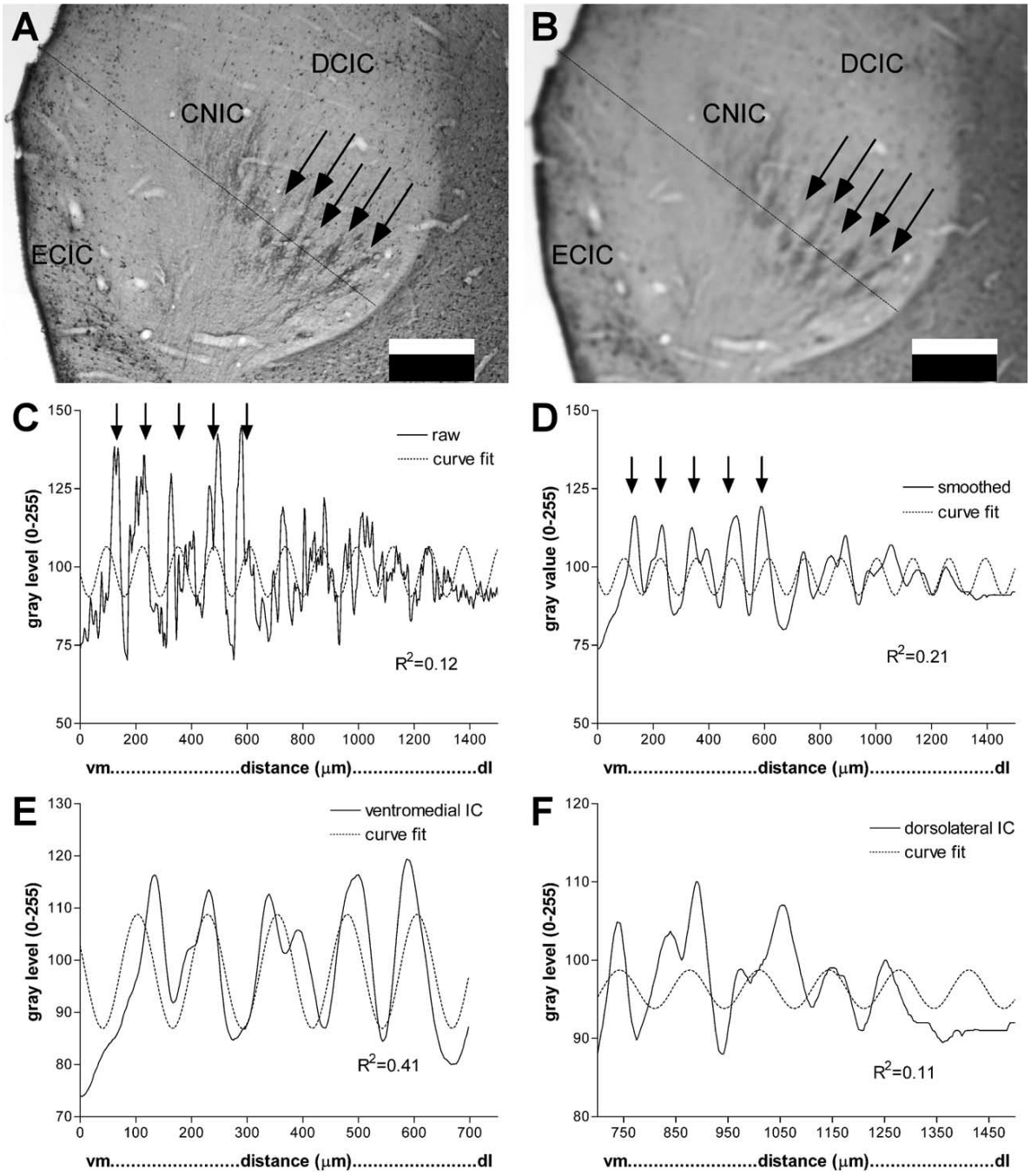

Fig 4.

Illustration of analysis of banded patterns in IC. Arrows indicate regions in CNIC of dense CB immunostained bands in low magnification images and corresponding peaks in line density plots (major subnuclei of IC are labeled in A and B for reference). (A) Raw gray level image of CB-immunostaining in P1 kitten IC showing a line selected for density analysis. The line begins at the vm and extends dl at approximately a right angle to the central layers of the immunostained plexus (2× objective). (B) The same image and line as in frame A, but the image has been smoothed with a Gaussian filter (Scion Image, 15×15 matrix). (C) Line density plot of gray levels (Scion Image) for the line in frame A. Dotted line is best sine curve fit (non-linear regression). Note the low goodness of fit (R^2=0.12). (D) Line density plot of gray levels

(Scion Image) for the line in the smoothed image in frame B. Dotted line is the best sine curve fit. Note the higher goodness of fit (R^2=0.21) compared with C. (E) Selected segment of line density analysis in frame D for the ventromedial region that is most banded. Dotted line is best sine curve fit for this regular periodic segment of the line plot. Note the high goodness of fit for this portion of the line density (R^2=0.41). (F) Selected segment of the line density analysis in frame D for the dorsolateral region is outside the best region of bands. Dotted line is best sine curve fit for this segment of the line plot. Note the low goodness of fit (R^2=0.11). Scale bars=0.5 mm for A, B; vm, ventromedial; dl, dorsolateral.

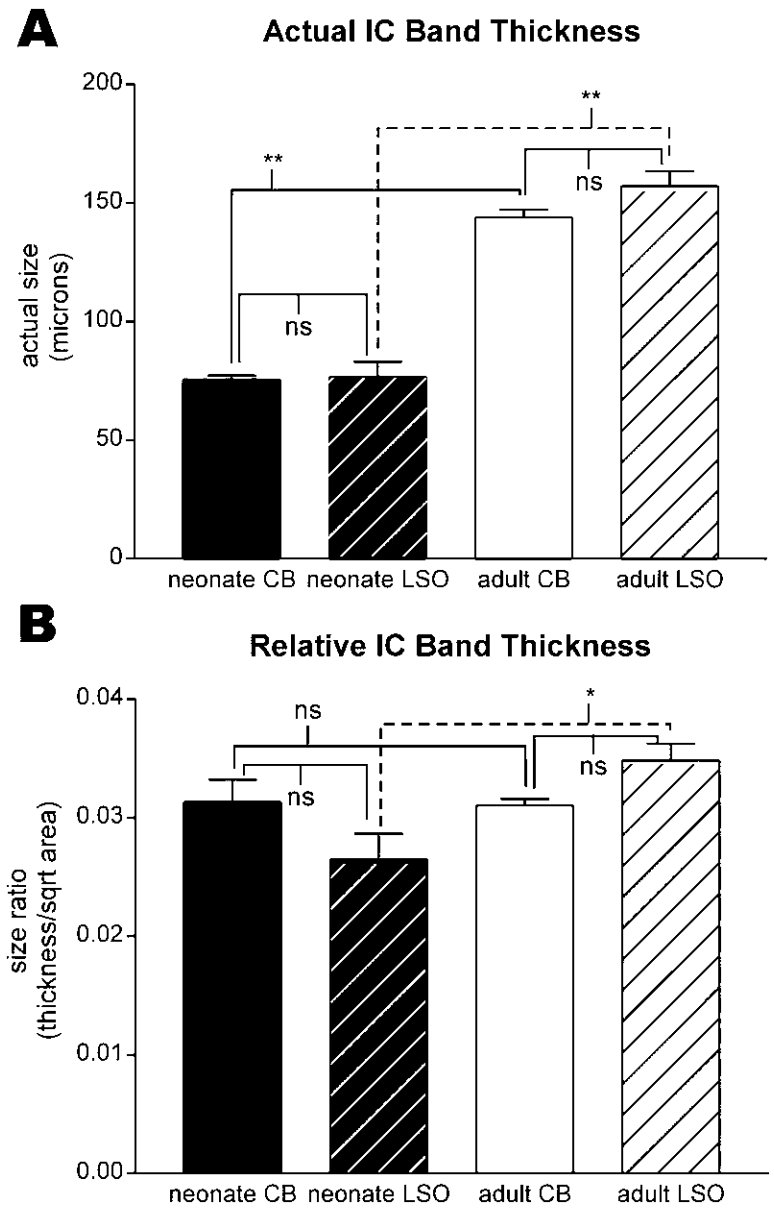

Fig 5.

Bar graphs comparing CB- and LSO-band thickness for neonate (black bars) and adult (white bars) IC. (A) Actual mean band thickness and standard deviation. There was no significant difference between thickness of neonate CB and LSO bands; similarly, there was no difference between thickness of adult CB and LSO bands. Both groups of neonate bands were significantly different from the corresponding adult group of bands. (B) Normalized band thickness mean and standard deviation. In contrast to actual band thickness, there was no significant difference between normalized neonate and adult CB band thickness nor between neonate CB and LSO band thickness, although neonate and adult LSO band thicknesses were just different (P=0.03). Brackets in A and B indicate results of Student's t-test comparing groups: * P value <0.05; **P value <0.005; ns, no significant difference.

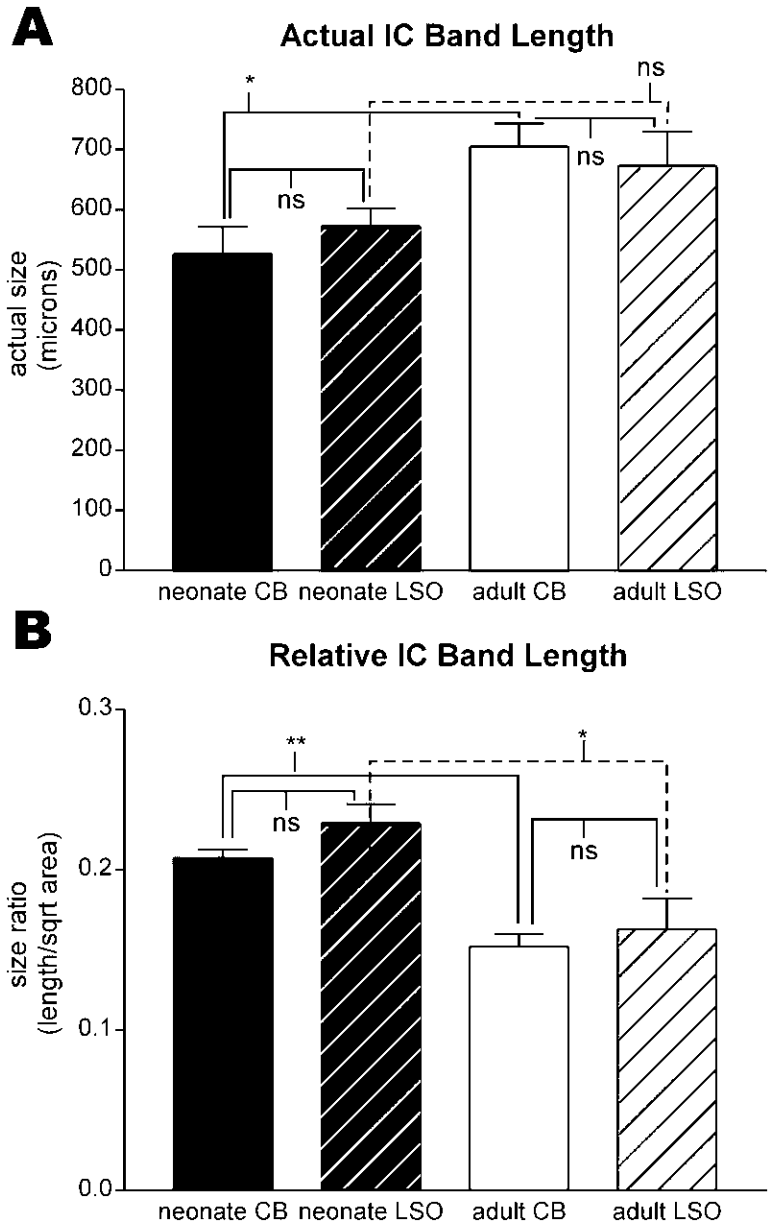

Fig 6.

Bar graphs comparing CB- and LSO-band length for neonate (black bars) and adult (white bars) IC. (A) Actual mean band length and standard deviation. Neonatal CB bands were shorter than adult CB bands (P=0.01) as were LSO bands (although P value for this sample was not quite significant). (B) Normalized mean band length and standard deviation. When normalized for IC growth, there was no difference in band length between neonatal CB and neonatal LSO bands or between adult CB and adult LSO bands. However, the normalized neonatal CB and LSO band were significantly longer than the respective adult bands. Brackets in A and B indicate results of Student's *t*-test comparing groups: * P value <0.05; ** P value <0.005; ns, no significant difference.

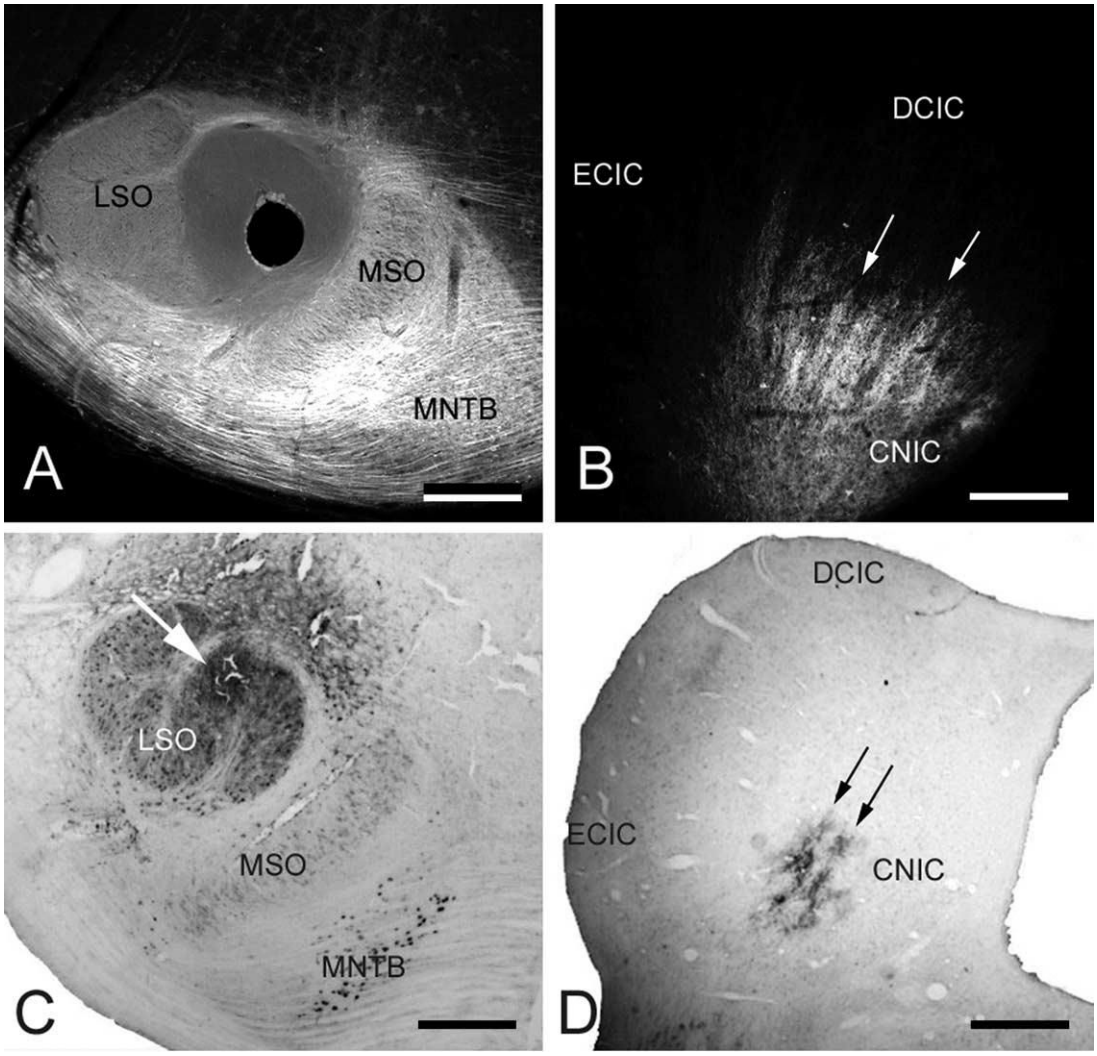

Fig 7.

Digital photomicrographs illustrating LSO tracer placements and labeled LSO projections to the ipsilateral CNIC. (A) Frontal section through P1 kitten superior olivary complex showing position of DiI-coated pin (hole) in the medial LSO. (B) Digital image of epifluorescent DiI-labeled axonal bands (arrows) in the CNIC. (C) Frontal section through adult cat superior olivary complex showing position of WGA-HRP injection (arrow) in medial LSO. (D) Brightfield digital photomicrograph of labeled axons ending in bands (arrows) in the CNIC. Scale bars=0.33 mm, A; 0.33 mm, B; 0.5 mm, C; 1 mm, D.